

pion triplet corresponding to the  $\omega$  cannot be identified, these events are not used in the present analysis; their distribution on the  $\omega$  Dalitz plot is discussed later.

<sup>7</sup>J. D. Jackson, J. T. Donohue, K. Gottfried, R. Keyser, and B. E. Y. Svensson, Phys. Rev. **134**, B428 (1965).

<sup>8</sup>See, for instance, the Aachen-Berlin-Birmingham-Bonn-Hamburg-London (I. C.)-München Collaboration, Phys. Rev. **138**, B897 (1965); H. O. Cohn, W. M. Bugg, and G. T. Condo, Phys. Letters **15**, 344 (1965); S. Goldhaber, J. L. Brown, I. Butterworth, G. Goldhaber, A. A. Hirata, J. A. Kadyk, and G. H. Trilling, Phys. Rev. Letters **15**, 737 (1965). See also Ref. 7.

<sup>9</sup>An attempt to determine spin and parity has been described by D. D. Carmony, R. L. Lander, C. Rindfleisch, N. Xuong, and P. Yager, Phys. Rev. Letters **12**, 254 (1964).

<sup>10</sup>If  $B$  has  $J^P = 1^-$ , one obtains a branching ratio  $\Gamma(B^\pm \rightarrow \pi^\pm + \pi^0) / \Gamma(B^\pm \rightarrow \pi^\pm + \omega) \approx 5$ , assuming equal coupling constants for these two decay modes. The cross section for  $\pi^- + p \rightarrow B^- + p$  with  $B^- \rightarrow \pi^- + \pi^0$  is estimated to be  $(0 \pm 20) \mu\text{b}$  based on 1940 events for the reaction  $\pi^- + p \rightarrow \pi^0 + \pi^- + p$  at 3.2 GeV/c (L. D. Jacobs, Lawrence Radiation Laboratory, private communication). At the same energy, the cross section for  $\pi^- + p \rightarrow B^- + p$  with  $B^- \rightarrow \pi^- + \omega$  based on our data is approximately  $(68 \pm 12) \mu\text{b}$  after correction for neutral decay of  $\omega$ .

<sup>11</sup>This feature can be seen more clearly with the 4.2-GeV/c data alone, where more phase space is available than at 3.2 GeV/c.

<sup>12</sup>M. Aderholz et al., Aachen-Berlin-Birmingham-Bonn-Hamburg-London (I. C.)-München Collaboration, Nuovo Cimento **35**, 659 (1965).

<sup>13</sup>B. E. Y. Svensson, Nuovo Cimento **37**, 714 (1965).

<sup>14</sup>For the inverse reaction  $\pi^- + p \rightarrow \rho^- + p$  at 1.25 GeV, E. Pickup, D. K. Robinson, and E. O. Salant, Phys. Rev. Letters **7**, 192 (1962), observed a strong peak at  $\cos\theta_{pp} = +1$ . The  $\pi^- p$  c.m. energy, 1.8 GeV, corresponds to the highest mass interval observed in the present experiment.

<sup>15</sup>Recent analyses have indicated that both the  $N^*(1518)$  and  $N^*(1688)$  are probably superpositions of several closely spaced resonances [P. Bareyre, C. Bricman, A. Stirling, and G. Villet, Phys. Letters **18**, 342 (1965)]. For additional evidence regarding isobar excitation by  $\rho$  exchange, we have investigated the reaction  $\pi^- + n \rightarrow p + \pi^- + \pi^-$  in deuterium at 3.2 GeV/c (to be published). Isobars (1238, 1518, 1688) are copiously produced at low  $\Delta p \pi^{-2}$ , suggesting  $\rho$  exchange. The distributions in  $\cos\theta_{pp}$  for  $N^{*0}(1518)$  and  $N^{*0}(1688)$  showed strong peaks near  $\cos\theta_{pp} = +1$ .

<sup>16</sup>The forward peak in  $\cos\theta_{pp}$  is associated with the  $B$  enhancement; consequently the nearly flat distribution of  $\cos\theta_{pp}$  in the region of  $N^*(1238)$  does not give rise to a strong  $B$  enhancement. The cluster of  $B$  events in  $N^*(1238)$  region in Fig. 1(c) results from the selection  $\Delta p^2 < 0.35 (\text{GeV}/c)^2$ ; this favors events in the region  $\cos\theta_{pp} = +1$ , which leads to an "exaggerated"  $B$  enhancement.

<sup>17</sup>M. A. Abolins, D. D. Carmony, R. L. Lander, N. Xuong, and P. M. Yager, in Proceedings of the Topical Conference on Resonant Particles, Ohio University, Athens, Ohio, 10-12 June 1965 (unpublished), p. 198, demonstrated that events in the final state  $\omega + N^{*++}(1238)$  made no substantial contribution to the  $B$  enhancement. The origin of the enhancement was not investigated for higher mass  $\pi^+ p$  systems.

<sup>18</sup>The central region of the Dalitz plot is defined by the condition  $r = |M|^2 / |M_{\text{max}}|^2 > 0.72$ , and the peripheral region by  $r < 0.72$ , where  $M$  is the matrix element for  $\omega$  decay, and  $M_{\text{max}}$  is its maximum value. With  $J^P = 1^-$ , equal numbers of  $\omega$  events are expected in the two regions ( $r = 0.72$  corresponds approximately to  $\lambda = 0.07$  defined in Ref. 2).

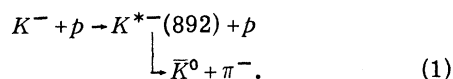
<sup>19</sup>In a recent compilation of  $\pi^\pm \omega$  data, not including the present data, the anomaly discussed in Ref. 2 is less pronounced (G. Goldhaber, private communication). Although double- $\omega$  events were included, the number of  $B$  events in the central and peripheral regions were compatible within two standard deviations.

## PRODUCTION AND DECAY PROPERTIES OF THE $K_0^*(892)$ PRODUCED IN THE REACTION $K^- + p \rightarrow \rho + \bar{K} + \pi^-$ AT 2.1, 2.45, AND 2.64 BeV/c\*

Jerome H. Friedman and Ronald R. Ross

Lawrence Radiation Laboratory, University of California, Berkeley, California  
(Received 7 February 1966)

We have measured the total cross section, differential cross section, and  $K^*(892)$  decay correlations for the reaction



Experimental decay distributions are consistent with the production and decay of a  $K^*$  relative-

ly free from interference with other processes. The 4300  $K^*$  events in the sample allowed us to determine the decay correlations as a function of production angle. Comparison of these correlations with simple meson-exchange models imply that pseudoscalar-meson exchange dominates the extreme forward direction, while vector-meson exchange seems to be responsible for the decay correlations at larger angles.

The data analyzed came from a sample of 100 000 events of the two-prong +  $V$  topology obtained in an exposure of the Lawrence Radiation Laboratory 72-inch  $H_2$  bubble chamber to a separated  $K^-$  beam of 2.1, 2.45, 2.58, 2.62, and 2.68 BeV/c.<sup>1</sup> Events of the type in Reaction (1) are four times overconstrained by the requirements of energy and momentum conservation. Less than 1% of these events were ambiguous with other physical hypotheses. In all, 7500 events of the type  $K^- + p - p + \bar{K}^0 + \pi^-$  resulted from the measurements, of which 7000 satisfied fiducial-volume and beam-track criteria and are used in the analysis.

We have divided the events into three beams momentum intervals with mean momenta 2.1, 2.45, and 2.64 BeV/c. Table I gives the number of events, the fraction of the events in which a  $K^*(892)$  is produced, and the cross sections for each momentum interval. More than 60% of the events in the lowest two beam momenta, and almost 60% in the upper, result from  $K^*$  production. Production of  $N^*(1238)$ ,  $N^*(1688)$ ,  $N^*(1512)$ ,  $Y_1^*(1660)$ , and  $Y_1^*(1765)$  are also observed, but at rates amounting to less than 10% in the most copious case, and

of order 2 to 3% on the average.

In analyzing the  $K^*$  production and decay properties, it has been customary to use events within a given  $(\bar{K}^0\pi^-)$  mass interval around the  $K^*$  mass. The mass interval is chosen as a compromise between minimizing contamination from non- $K^*$  events and minimizing statistical errors. One is forced to include some "background" events. The assumption of noninterference of background amplitudes with the  $K^*$  production and decay amplitudes is essential for this analysis, but even the "noninterfering background" will cause errors in the determination of the  $K^*$  decay parameters.

We have avoided the arbitrariness of limits on the mass cut and allowed for the effect of noninterfering background by using the maximum-likelihood method and a simple model of noninterfering production rates to determine simultaneously the amount of all known resonances produced, the  $K^*$  decay correlation coefficients, and the amount of nonresonant background. Decay correlations of other resonances produced were not included primarily because of their small rate of production. The frequency function used for each event has the form

$$P(x, \hat{k}; r, a, b, c) = \sum_i \frac{r_i}{N_i} \text{BW}(E_i, \Gamma_i; X_i) + \frac{1 - \sum_i r_i}{N_p} + \frac{1}{N_{K^*}} \text{BW}(E_{K^*}, \Gamma_{K^*}; X_{\bar{K}^0\pi^-}) [r_{K^*} + a Y_2^0(\hat{k}) + b \text{Re} Y_2^1(\hat{k}) + c \text{Re} Y_2^2(\hat{k})]. \quad (2)$$

Here  $r_i$  is the relative rate of production of the  $i$ th resonance;  $N_i$  is the total phase space for the  $i$ th resonance; BW is a Breit-Wigner function of the mass  $E_i$  and width  $\Gamma_i$  of the  $i$ th resonance and of the appropriate effective-mass combination  $X_i$  of the event;  $N_p$  is the total three-body phase space for the event;  $Y_l^m(\hat{k})$  is a spherical harmonic whose argument,  $\hat{k}$ , is a unit vector in the direction<sup>2</sup> of the  $\pi^-$ ; and  $a$ ,  $b$ , and  $c$  are the decay correlation coefficients of the  $K^*$  and are related to the  $K^*$  spin-

Table I. Number of events and cross sections as a function of momentum. Cross-section determinations include corrections applied to the observed numbers of events for neutral decay modes of  $\bar{K}^0$  (3.0) as well as the fiducial-volume escape and short-length  $\bar{K}^0$  (1.06).

Momentum (BeV/c)	Number of events $K^- + p \rightarrow p + \bar{K}^0 + \pi^-$	% $K^*(892)$ in		Total cross section (mb)	
		$K^- + p \rightarrow p + \bar{K}^0 + \pi^-$	$K^- + p \rightarrow p + \bar{K}^0 + \pi^-$	$K^- + p \rightarrow p + \bar{K}^0 + \pi^-$	$K^- + p \rightarrow K^{*-} + p$
2.1	2340	65.3 ± 1.8		2.05 ± 0.10	1.34 ± 0.08
2.45	926	61.2 ± 2.6		1.79 ± 0.10	1.10 ± 0.08
2.64	3727	57.6 ± 1.2		1.45 ± 0.09	0.83 ± 0.05

density matrix elements by the formulas

$$\rho_{00} = \frac{1}{3} + \frac{\sqrt{5}}{3} \frac{a}{(4\pi)^{1/2} r_{K^*}}; \quad \rho_{1-1} = -\frac{(30)^{1/2}}{12} \frac{c}{(4\pi)^{1/2} r_{K^*}};$$

$$\text{Re}\rho_{10} = \frac{(15)^{1/2}}{12} \frac{b}{(4\pi)^{1/2} r_{K^*}}.$$

In Eq. (2) we have neglected the "illegal" decay correlations of the  $K^*$ , i.e., those prohibited by angular-momentum and parity conservation. This assumes that the  $K^*$  decays as a free particle and that there is no interference between the  $K^*$  production and decay and other processes.

To determine the production angular distribution and decay correlation coefficients as a function of production angle, we divided the data at each momentum into intervals in the production angle of the  $\bar{K}^0\pi^-$  system. The intervals were chosen to include approximately 100  $K^*$  events in each. Maximum-likelihood solutions were obtained for each of these intervals. Figure 1 and Table II give the results of these solutions for 2.1, 2.45, and 2.64 BeV/c.

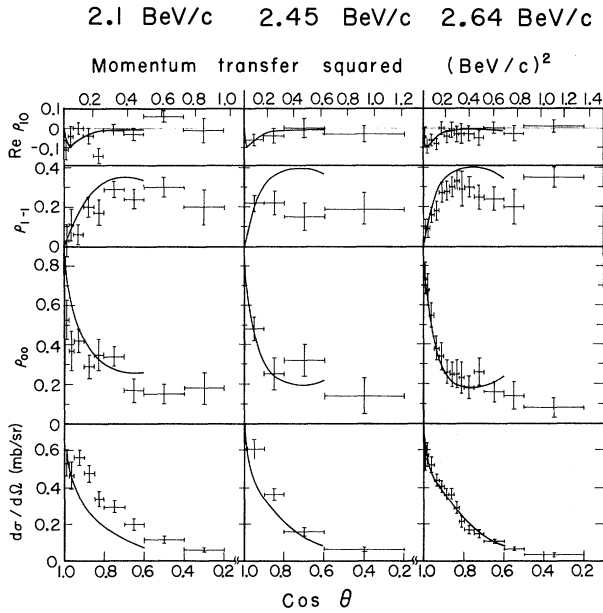


FIG. 1. Differential cross section and spin-density-matrix elements as a function of production angle for the three momentum intervals. The solid curves are predictions of the absorption model based on a fit to the differential scattering cross section at 2.64 BeV/c.<sup>6,7</sup>

Since the maximum-likelihood solutions are based on a model not necessarily representative of the data, we compare the solutions to the data in Figs. 2 and 3. Events selected for these plots were required to have an effective  $\bar{K}^0\pi^-$  mass in the range 0.816 to 0.976 BeV, in addition to the  $\bar{K}^0\pi^-$  production angular interval indicated. This mass cut has introduced an estimated fraction of background events amounting to 5% at the most forward  $\cos\theta$  intervals and 25% at the most backward. The distributions shown refer only to the decay of the  $K^*$ , but these distributions should be quite sensitive to the effects of interference between the  $K^*$  production and decay amplitude and other amplitudes. Specifically, any asymmetries with respect to reflection about  $\varphi = 0$  and  $180^\circ$  or, after averaging over  $\varphi$ , about  $\cos\alpha = 0$  are not accounted for in our model.

Figure 2 contains plots of the decay distribution of the  $K^*$  with respect to the cosine of the polar angle  $\alpha$  and to the azimuthal angle  $\varphi$  for the indicated production angle intervals and incident  $K^-$ -beam momenta. The solid curves are predictions of the likelihood solutions which take the form

$$I(\cos\alpha) = N \times \frac{3}{2} [\rho_{00} \cos^2\alpha + \frac{1}{2}(1-\rho_{00}) \sin^2\alpha],$$

and

$$I(\varphi) = (N/2\pi)[1 - 2\rho_{1-1} \cos 2\varphi],$$

where  $N$  normalizes to the number of events in the plot. The over-all agreement between the solutions and the data is quite good. The data at 2.64 and 2.45 BeV/c show no significant asymmetries. Only the plot for  $-1 \leq \cos\theta \leq 0.2$  at 2.1 BeV/c shows a marked asymmetry. It is not clear whether this asymmetry in the events is attributable to a failure of the model or due to a symmetric  $K^*$  distribution plus an asymmetric noninterfering background.

Figure 3 contains scatter plots of  $\cos\alpha$  vs  $\varphi$  for three judiciously chosen samples of events. The parameter of the model being tested here is primarily  $\text{Re}\rho_{10}$  through its contribution to the intensity of the  $K^*$  decay:

$$I(\cos\alpha, \varphi) = (3/4\pi) [\rho_{00} \cos^2\alpha + \frac{1}{2}(1-\rho_{00}) \sin^2\alpha - \rho_{1-1} \sin^2\alpha \cos 2\varphi - \sqrt{2} \text{Re}\rho_{10} \sin 2\alpha \cos \varphi].$$

The plots of Fig. 2 are independent of this parameter, since the average values of  $\cos\varphi$  over  $\varphi$  and of  $\sin 2\alpha$  over  $\alpha$  are both zero.

Since  $\text{Re}\rho_{10}$  is small, the density of events is primarily determined by the  $\rho_{00}$  and  $\rho_{1-1}$  terms; however the shift of contours of equal intensity as a function of  $\varphi$  is apparent in all three plots, and the events follow these shifts. Figure 3(a) contains events at all momenta and all production angles, serving as an over-all check on the solutions. Events on Fig. 3(b) and 3(c) were chosen to illustrate regions where  $\cos^2\alpha$  and  $\sin^2\alpha$  terms were dominant, respectively.

The consistency between the data and the

likelihood solution based on our simple model suggest that the  $K^*$  produced in the reaction studied here is essentially free from interference, and can be used to test theoretical models of production and decay which assume production of a free  $K^*$ .

Qualitative features of the decay distributions of Fig. 2 for the 2.64-BeV/c data show the following: (a) In the extreme forward direction ( $0.95 \leq \cos\alpha \leq 1$ ), there is a strong  $\cos^2\alpha$  polar distribution and a somewhat flat

Table II. Number of events, differential cross section, and spin-density matrix elements of  $K^*(892)$  as a function of production angle.

Cos $\theta$ interval	Number of $K^*(892)$	$d\sigma/d\Omega$ (mb/sr)	$\rho_{00}$	$\rho_{1-1}$	$\text{Re}\rho_{10}$
A. 2.1 BeV/c					
0.975 to 1	96 ± 13	0.53 ± 0.07	0.53 ± 0.10	0.03 ± 0.08	-0.11 ± 0.05
0.95 to 0.975	84 ± 12	0.46 ± 0.07	0.37 ± 0.10	0.11 ± 0.08	-0.04 ± 0.05
0.9 to 0.95	203 ± 16	0.56 ± 0.04	0.42 ± 0.06	0.06 ± 0.05	0.00 ± 0.03
0.85 to 0.9	172 ± 15	0.47 ± 0.04	0.29 ± 0.06	0.20 ± 0.05	-0.04 ± 0.04
0.8 to 0.85	121 ± 13	0.34 ± 0.04	0.35 ± 0.08	0.17 ± 0.06	-0.14 ± 0.04
0.7 to 0.8	214 ± 17	0.30 ± 0.03	0.34 ± 0.05	0.29 ± 0.04	-0.01 ± 0.03
0.6 to 0.7	142 ± 14	0.20 ± 0.03	0.17 ± 0.06	0.24 ± 0.05	-0.03 ± 0.03
0.4 to 0.6	172 ± 15	0.12 ± 0.02	0.15 ± 0.05	0.30 ± 0.05	0.06 ± 0.03
0.2 to 0.4	91 ± 12	0.06 ± 0.01	0.18 ± 0.08	0.20 ± 0.09	-0.01 ± 0.06
-0.2 to 0.2	124 ± 15	0.04 ± 0.01	0.00 ± 0.06	0.00 ± 0.08	0.02 ± 0.05
-1 to -0.2	124 ± 16	0.03 ± 0.01	0.20 ± 0.09	0.11 ± 0.08	-0.14 ± 0.05
-1 to 1	1528 ± 53 <sup>a</sup>	0.106 ± 0.006	0.255 ± 0.020	0.155 ± 0.018	-0.034 ± 0.011
B. 2.45 BeV/c					
0.9 to 1	199 ± 16	0.60 ± 0.05	0.48 ± 0.06	0.22 ± 0.04	-0.06 ± 0.03
0.8 to 0.9	120 ± 13	0.36 ± 0.03	0.25 ± 0.08	0.22 ± 0.06	-0.04 ± 0.04
0.6 to 0.8	103 ± 12	0.16 ± 0.02	0.32 ± 0.08	0.15 ± 0.07	0.00 ± 0.05
0.2 to 0.6	86 ± 11	0.06 ± 0.01	0.14 ± 0.09	0.19 ± 0.08	-0.03 ± 0.04
-0.2 to 0.2	45 ± 9	0.01 ± 0.01	0.04 ± 0.12	0.26 ± 0.11	0.06 ± 0.06
-1 to -0.2	28 ± 9	0.005 ± 0.01	0.00 ± 0.17	0.09 ± 0.20	-0.22 ± 0.10
-1 to 1	596 ± 32 <sup>b</sup>	0.087 ± 0.006	0.280 ± 0.033	0.230 ± 0.029	-0.039 ± 0.018
C. 2.64 BeV/c					
0.9875 to 1	113 ± 14	0.55 ± 0.06	0.74 ± 0.08	0.09 ± 0.05	-0.05 ± 0.05
0.975 to 0.9875	117 ± 13	0.57 ± 0.06	0.68 ± 0.08	0.09 ± 0.05	-0.09 ± 0.04
0.95 to 0.975	214 ± 17	0.52 ± 0.04	0.55 ± 0.06	0.16 ± 0.04	-0.06 ± 0.03
0.925 to 0.95	179 ± 15	0.43 ± 0.03	0.38 ± 0.06	0.18 ± 0.05	-0.08 ± 0.03
0.9 to 0.925	166 ± 15	0.40 ± 0.03	0.34 ± 0.07	0.27 ± 0.05	0.00 ± 0.03
0.875 to 0.9	150 ± 14	0.36 ± 0.03	0.26 ± 0.06	0.28 ± 0.05	-0.04 ± 0.03
0.85 to 0.875	148 ± 14	0.36 ± 0.03	0.25 ± 0.06	0.30 ± 0.05	-0.01 ± 0.04
0.825 to 0.85	119 ± 12	0.28 ± 0.03	0.25 ± 0.07	0.33 ± 0.05	-0.03 ± 0.04
0.8 to 0.825	88 ± 11	0.21 ± 0.03	0.23 ± 0.08	0.29 ± 0.09	-0.03 ± 0.05
0.75 to 0.8	144 ± 14	0.17 ± 0.02	0.18 ± 0.06	0.30 ± 0.05	-0.03 ± 0.04
0.7 to 0.75	124 ± 12	0.15 ± 0.02	0.26 ± 0.07	0.25 ± 0.06	-0.05 ± 0.04
0.6 to 0.7	161 ± 15	0.11 ± 0.01	0.16 ± 0.05	0.24 ± 0.06	0.00 ± 0.03
0.5 to 0.6	108 ± 12	0.06 ± 0.01	0.14 ± 0.07	0.20 ± 0.09	-0.03 ± 0.04
0.2 to 0.5	183 ± 16	0.03 ± 0.01	0.08 ± 0.05	0.35 ± 0.05	0.01 ± 0.03
-0.2 to 0.2	121 ± 13	0.02 ± 0.01	0.00 ± 0.05	0.31 ± 0.07	-0.03 ± 0.02
-1 to -0.2	61 ± 12	0.01 ± 0.01	0.00 ± 0.15	0.31 ± 0.13	-0.01 ± 0.07
-1 to 1	2147 ± 57 <sup>c</sup>	0.066 ± 0.003	0.259 ± 0.017	0.252 ± 0.014	-0.035 ± 0.009

<sup>a</sup>Sum of column 2 = 1543

<sup>b</sup>Sum of column 2 = 581

<sup>c</sup>Sum of column 2 = 2196

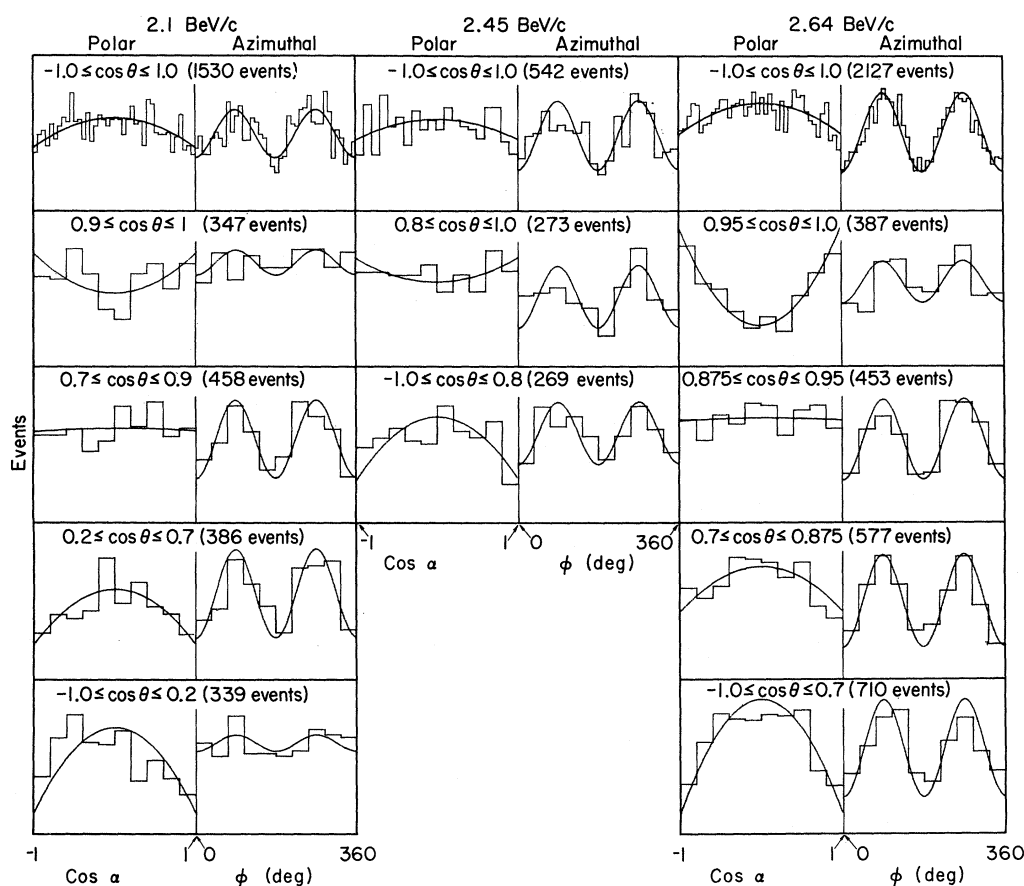


FIG. 2. Polar cosine and azimuthal decay-angle distributions of the  $K^*(892)$  at 2.1, 2.45, and 2.64 BeV/c for various intervals in production angle. The coordinate system is defined in the text.<sup>2</sup> The events plotted have a  $\bar{K}^0\pi^-$  effective mass between 0.816 and 0.976 BeV. The solid curves are the distributions predicted by the maximum-likelihood solution employing only "legal" moments.

azimuth distribution. This is characteristic of pseudoscalar exchange in the production process. (b) In the intermediate ( $0.7 \leq \cos\alpha \leq 0.875$ ) and backward ( $-1 \leq \cos\alpha \leq 0.7$ ) directions there are strong  $\sin^2\alpha$  polar distributions and  $1 - a \cos 2\phi$  azimuth distributions, characteristic of vector exchange. (c) In the plot for  $0.875 \leq \cos\theta \leq 0.95$ , there is a relatively flat polar distribution and a moderate  $1 - a \cos\phi$  azimuth distribution, which may result from a combination of pseudoscalar and vector exchange. Although somewhat more limited in statistics, the data at 2.1 and 2.45 BeV/c exhibit the same general features. These qualitative features of the data have been predicted by Jackson *et al.*<sup>3</sup> using a meson-exchange model with corrections for initial- and final-state absorptions.

In fitting the  $K^{*+}$ -production differential cross section in the reaction  $K^+ + p \rightarrow K^{*+} + p$ ,<sup>4</sup> Jack-

son *et al.* found two possible solutions that fit the data equally well. Solution I gave destructive interference in the forward direction between the pion and vector-exchange amplitudes and solution II gave constructive interference. Using the vector coupling constants determined from the  $K^+$  data and absorption parameters appropriate to the reaction  $K^- + p \rightarrow K^{*-} + p$ , they compared their result to  $K^{*-}$  production and decay at 3 BeV/c.<sup>5</sup> Both solutions predicted the spin-density matrix elements within errors, but predicted a  $d\sigma/d\Omega$  that was about 50% too small. Jackson and Donohue<sup>6</sup> have determined a new set of parameters<sup>7</sup> in the region of their old solution II by fitting to the differential cross section at 2.64 BeV/c shown in Fig. 1. No acceptable values of  $\xi$  and  $\eta$  could be found for parameters in the region of solution I. Using the new set of parameters they have calculated all the solid curves drawn

over the data of Fig. 1. The over-all agreement is remarkably good considering the small number of parameters entering into the theory and the fact that the only information fed

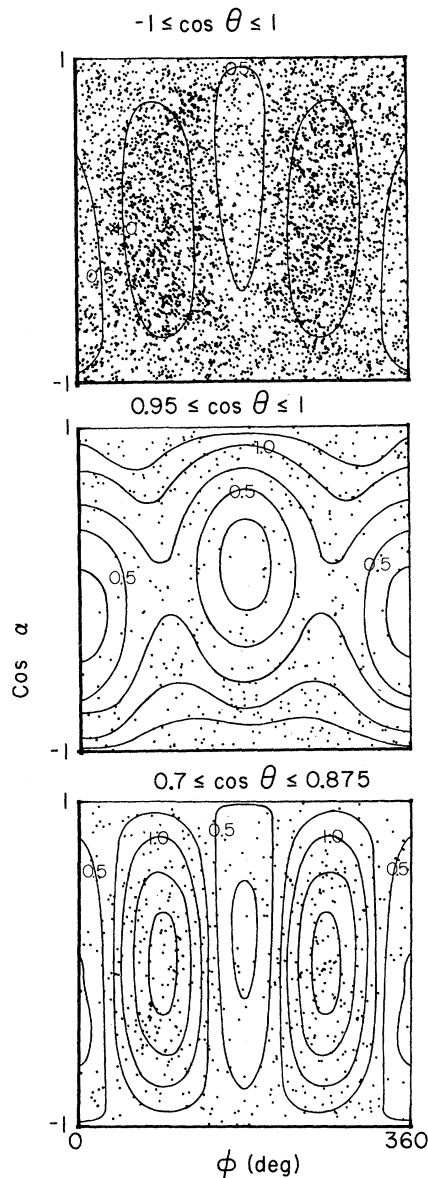


FIG. 3. Scatter plots of polar cosine versus azimuth angle (a) for all events summed over all production angles and beam momenta, (b) for 2.64 BeV/c, with  $0.95 \leq \cos \theta \leq 1.0$ , illustrating a region most dominated by a large  $\cos^2 \alpha$  term, and (c) for 2.64 BeV/c, with  $0.7 \leq \cos \theta \leq 0.875$ , illustrating a region dominated by a large  $\sin^2 \alpha$  term. The solid lines are lines of equal relative intensity predicted by the solutions given in Table II for (b) and (c). For (a) the parameters are the appropriate average of the parameters in the last row of Table II.

in is the differential-scattering cross section. At 2.64 BeV/c, the fit to the differential cross section is very good and the predictions are also quite acceptable for  $\rho_{00}$  and  $\text{Re}\rho_{10}$ . The theoretical curve seems to systematically overestimate  $\rho_{1-1}$  by a standard deviation or so. The same seems to be true for 2.45 BeV/c except that the theoretical curve underestimates the differential cross section slightly although giving good agreement as to its shape. At 2.1 BeV/c, the agreement of the theoretical curves with the spin-density matrix elements is acceptable; however, the underestimation of the differential cross section is much more exaggerated. This difficulty in predicting absolute cross sections for  $K^*$  production as a function of energy, where vector exchange is involved, has already been found by Jackson *et al.*<sup>3</sup> in comparing  $K^+p$  data at 3 and 5 BeV/c. Reasons have been advanced to explain why the absorption model should not work for vector exchange,<sup>3,8</sup> but as yet no satisfactory model has been advanced to take its place.

In summary, Fig. 1 and Table II contain our measurements of the production and decay properties of the  $K^{*-}$  in  $K^-p$  interactions at 2.1, 2.45, and 2.64 BeV/c. Because of the agreement in Figs. 2 and 3 between the data and the likelihood solutions based on a free- $K^*$  model, we believe the  $K^*$  is produced and decays without significant interference with other processes. The absorption model is capable of representing the qualitative features of the decay of the  $K^*$  but fails, again, to predict energy dependence of the total production cross section.

We acknowledge the support and cooperation of many members of the Alvarez group. We thank Professor Luis Alvarez for his continued encouragement and support. We are indebted to J. D. Jackson and J. T. Donohue for useful discussions and for the theoretical curves of Fig. 1. We acknowledge with thanks the efforts of the people who helped with the scanning and measuring, and of the 72-inch bubble chamber and Bevatron operating crews.

\*Work sponsored by the U. S. Atomic Energy Commission.

<sup>1</sup>J. J. Murray, J. Button-Shafer, F. T. Shively, G. H. Trilling, J. A. Kadyk, A. Rittenberg, D. M. Siegel, J. S. Lindsey, and D. Merrill, "A Separated 2.5- to

2.8-GeV/c  $K^-$  Beam at the Bevatron," presented at the Proceedings of the Conference on High-Energy Physics, Dubna, 5-15 August 1964 (to be published); Lawrence Radiation Laboratory Report No. UCRL-11426, 1964 (unpublished).

<sup>2</sup>The coordinate system in the rest frame of the  $K^*$  for its decay is chosen so that the polar axis is in the direction of the incident  $K^-$ , and the  $y$  axis is the normal to the production plane defined by  $\hat{n} = (\hat{p}' \times \hat{K}^-) / |\hat{p}' \times \hat{K}^-|$ . Here  $\hat{p}'$  is a unit vector in the direction of the final-state proton, and  $\hat{K}^-$  is a unit vector in the direction of the  $K^-$ . The  $x$  axis is then chosen so as to make a right-handed coordinate system.

<sup>3</sup>J. D. Jackson, J. T. Donohue, K. Gottfried, R. Keyser, and B. E. Y. Svensson, Phys. Rev. **139**, B428 (1965).

<sup>4</sup>G. R. Lynch, M. Ferro-Luzzi, R. George, Y. Goldschmidt-Clermont, V. P. Henri, B. Jongejans, D. W. G. Leith, F. Muller, and J. M. Perreau, Phys. Letters

**9**, 359 (1964).

<sup>5</sup>R. Barloutaud, A. Leveque, C. Louedec, J. Meyer, P. Schlein, A. Verglas, J. Badier, M. Demoulin, J. Goldberg, B. P. Gregory, P. Krejbich, C. Pelletier, M. Ville, E. S. Gelsema, J. Hoogland, J. C. Kluyver, and A. G. Tenner, Phys. Letters **12**, 352 (1964).

<sup>6</sup>J. D. Jackson and J. T. Donohue, private communication. These calculations differ from those of Ref. 3 in that exact partial-wave sums are used instead of the Bessel-function approximations.

<sup>7</sup>In the notation of Ref. 3, the values of the parameters that were used to construct the distribution in Fig. 1 are  $\xi = -1.8$  and  $\eta = -1.1$ . Choosing values of  $\xi$  and  $\eta$  along the line  $2.2\xi - \eta = -2.9$  changes the fit to  $d\sigma/d\Omega$  very little but does change the curves for  $\rho_{00}$ , etc. The values chosen are those giving the best representation of the spin-density-matrix elements.

<sup>8</sup>J. S. Ball and W. R. Fraser, Phys. Rev. Letters **14**, 746 (1965).

SEARCH FOR DISCRETE SOURCES OF COSMIC GAMMA RAYS ABOVE 1 GeV\*

H. B. Ögelman, J. P. Delvaille, and K. I. Greisen

Laboratory of Nuclear Studies, Cornell University, Ithaca, New York

(Received 16 February 1966)

At the present it is widely believed that the flux received from nonthermal radio sources is due to synchrotron radiation emitted by high-energy electrons ( $10^9$  to  $10^{12}$  eV) spiraling in the weak magnetic fields ( $10^{-3}$  to  $10^{-6}$  G) of the sources. It has further been suspected that the dominant mode of electron production is the decay of charged mesons that are created by nuclear interactions of high-energy protons.<sup>1-4</sup> An immediate consequence of this speculation is that there should be a comparable amount of high-energy gamma radiation produced as the decay product of the neutral mesons. In addition, it is also plausible that gamma rays could be produced through bremsstrahlung and inverse Compton effect with visible light of the high-energy electrons in the sources.<sup>5-7</sup> It is of great interest to detect these gamma rays and obtain direct information about the validity of the above suppositions.

Calculations of the expected flux of gamma rays above 1 GeV due to the above-mentioned mechanisms range from  $10^{-4}$  to  $10^{-8}$  photons/cm<sup>2</sup> sec at the earth. Experiments in search of high-energy gamma rays (50 MeV to 1 GeV) have already been reported.<sup>8-18</sup> Although some yielded measurements of the isotropic background, no convincing discrete sources of gam-

ma rays were observed; upper limits were given for sources of interest.

In the experiment reported here we have attempted to detect sources of cosmic gamma rays above 1 GeV with a balloon-borne instrument. A schematic cross section of the apparatus is shown in Fig. 1. It consisted of a pair of sonic spark chambers, 850 cm<sup>2</sup> in area and separated by 22.5 cm, which recorded the direction of the pair formed after conversion

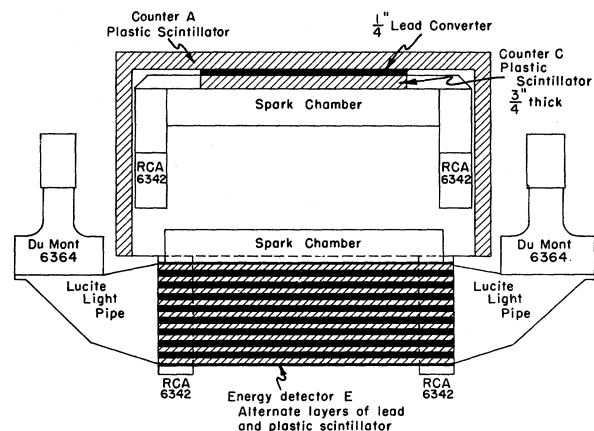


FIG. 1. A schematic cross section of the detector system.